Routes to Conjugated Polymers with Ferrocenes in Their Backbones: Synthesis and Characterization of Poly(ferrocenylenedivinylene) and Poly(ferrocenylenebutenylene)

Colby E. Stanton, T. Randall Lee,† Robert H. Grubbs,* and Nathan S. Lewis*

Division of Chemistry and Chemical Engineering,‡ California Institute of Technology, Pasadena, California 91125

John K. Pudelski and Matthew R. Callstrom

Department of Chemistry, The Ohio State University, Columbus, Ohio 43210

Mark S. Erickson and Mark L. McLaughlin

Department of Chemistry, Louisiana State University, Baton Rouge, Louisiana 70803

Received June 27, 1995; Revised Manuscript Received August 3, 1995⊗

ABSTRACT: Ring opening metathesis polymerization (ROMP) has been used to prepare conjugated polymers that contain ferrocene moieties as part of their backbones. The conjugated polymer poly(ferrocenylenedivinylene) (PFDV) and the analogous unconjugated polymer poly(ferrocenylenebutenylene) (PFB) with chain lengths of greater than 10 were found to be insoluble in typical organic solvents. The conductivities of oxidatively doped films of PFDV and PFB were found to be 10^{-4} and 10^{-5} Ω^{-1} cm^{-1}, respectively. Oxidative doping of the monomer 1,4-(1,1′-ferrocenediyl)-1-butene was found to yield conductivities on the order of 10^{-5} Ω^{-1} cm^{-1}, supporting interchain hopping as the dominant mechanism for charge carrier movement through these films. The ROMP of monomers octamethyl-1,4-(1,1′-ferrocenediyl)-1,3-butadiene and 1,4-(1,1′-ferrocenediyl)-1-methoxy-1,3-butadiene was also studied. Although soluble polymer was successfully generated from the latter monomer, no conditions were found under which the octamethyl compound could be polymerized.

I. Introduction

Interest in the incorporation of transition metals into the backbones of organic polymers has been sparked by the possibility of designing processable organometallic polymers that exhibit useful opto-electrical properties.[1] This approach would ideally combine the electrical conductivity and stability of metals with the elasticity, strength, and processability of organic polymers. Specifically, conjugated polymers that contain transition metals in their backbones represent an interesting and potentially useful class of these materials for use in applications such as solar energy conversion systems.[2] However, previous attempts to synthesize such conjugated polymers have yielded materials that suffer from poor solubilities and conductivities, in addition to low molecular weights.[3]

Ferrocenes have been attractive moieties for incorporation into the backbones of conducting organic polymers. It was anticipated that the ferrocene linkages would add flexibility to the conjugated chains by functioning as rotatable π-bonds. This flexibility might lend solubility and therefore processability to the polymers.[4] Also, since ferrocenes are thermally robust (>500 °C) and air stable,[5] conjugated polymers containing ferrocenes in the backbones were expected to be similarly robust. In addition, the functionalization of ferrocenes is well-developed;[6] thus, it was believed that substituted ferrocene-containing monomers might easily be synthesized and could provide routes to polymers with specific electronic properties.

The research teams headed by Manners[7–14] and Pannell[15–17] have reported the successful polymerization of [1]ferrocenophanes with a silicon atom bridge (*e.g.*, **1**) as well as a few germanium and phosphorus ana-

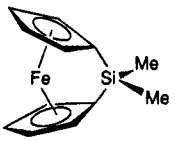

1

logues. These [1]ferrocenophanes possess structures with sufficient strain to allow effective thermal polymerization. This process has yielded high molecular weight organometallic polymers, **2**. Attempts to extend

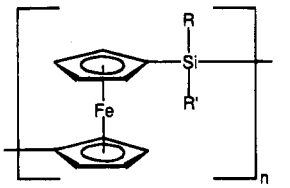

2

this thermal polymerization methodology to the analogous ferrocenophanes, **3**, with two Si atoms in the bridge, were unsuccessful. This failure probably reflects

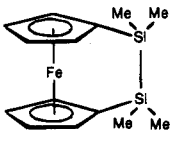

3

* To whom correspondence should be addressed.
† NIH Postdoctoral Fellow. Present address: Department of Chemistry, University of Houston, Houston, TX 77204-5641.
‡ Contribution No. 8967.
⊗ Abstract published in *Advance ACS Abstracts,* October 1, 1995.

0024-9297/95/2228-8713$09.00/0

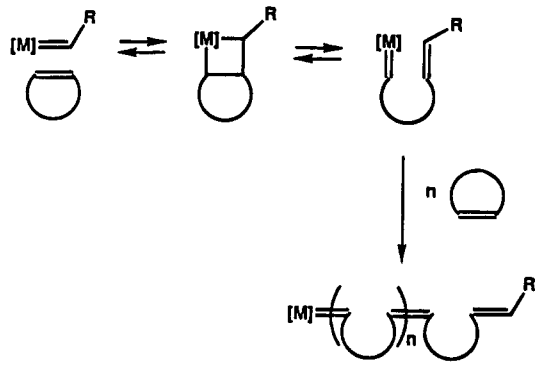

Figure 1. Ring opening metathesis polymerization, or ROMP, which utilizes a transition metal carbene catalyst that forms a metallacycle intermediate from a cyclic olefin. Productive cleavage of this metallacycle and subsequent steps lead to the formation of polymer. For an excellent introduction to the ROMP mechanism, as well as other polymerization routes, see refs 19 and 20.

the lower degree of ring strain in this latter class of compounds.[9,16] Interestingly, Manners and co-workers found that the analogous hydrocarbon-bridged [2]ferrocenophane **4**, which is considerably more strained than **3**,[18] readily undergoes thermal ring-opening polymerization. By heating compound **4**, which consisted of a complex mixture of isomers, to 300 °C in an evacuated, sealed Pyrex tube, high molecular weight polymeric material was obtained (eq 1).[18] These results showed that it is possible to synthesize polymers by the thermal cleavage of ferrocenophanes.

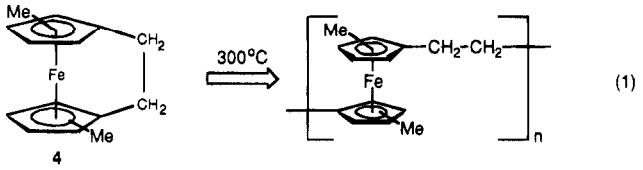

(1)

While the aforementioned experiments produced high molecular weight polymers containing ferrocene moieties in their backbones, none possessed the extended conjugation necessary for electrically conductive polymers. In an effort to develop a new route to processable conjugated polymers with ferrocene moieties comprising parts of their backbones, this manuscript describes the ring-opening metathesis polymerization (ROMP) of conjugated unsaturated ferrocenophanes (eq 2). This

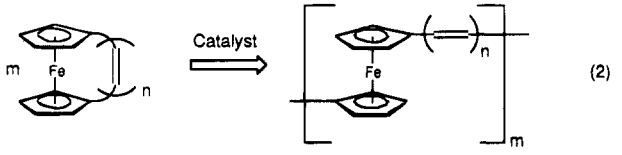

(2)

methodology employed a transition metal carbene catalyst to polymerize cyclic olefins (Figure 1).[19,20] The three ROMP catalysts that were used in these studies are

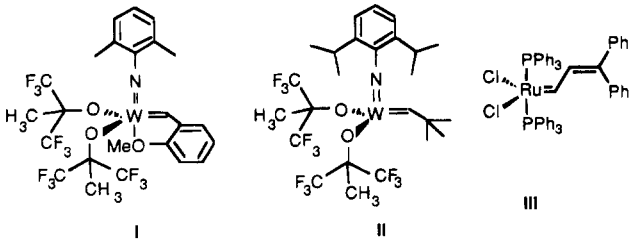

ROMP was chosen for a number of reasons as a promising route to conjugated organometallic polymers. First, ROMP is ideal for the synthesis of conjugated polymers, as the number of double bonds in the monomer is conserved in the polymer. Second, the molecular weight distribution of polymers produced by ROMP is remarkably narrow,[20-23] and the average molecular weights (*i.e.*, the number of monomers in each polymeric chain) are easily controlled.[24,25] Third, certain ROMP catalysts can tolerate a wide range of chemical functionalities and reaction conditions,[25-27] thus it should be possible to tune the electronic properties of conjugated polymers by appropriately incorporating heteroatomic substituents in the monomers. Finally, block copolymers with monodispersed segments and/or polymers with specific end groups can be synthesized using the ROMP methodology.[28,29]

Initial studies described in this work focused on the ROMP of 1,4-(1,1′-ferrocenediyl)-1,3-butadiene, **5**, to generate the conjugated polymer poly(ferrocenylenedivinylene) (PFDV), **6** (eq 3). As stated previously, it was

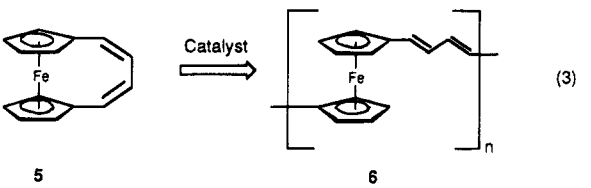

(3)

believed that the ferrocene group in PFDV would be able to rotate, making the polymer soluble and therefore processable. Furthermore, the $p\pi-d\pi$ conjugation in PFDV would potentially provide this polymer with attractive electrical features, such as a high conductivity when oxidatively doped.

In a related study, poly(ferrocenylenebutenylene) (PFB), a nonconjugated analogue of PFDV, was to be generated by ROMPing monomer **7** (eq 4). A comparison of the conductivity of the conjugated poly(ferrocenylene divinylene) **6** with that of the nonconjugated poly(ferrocenylenebutenylene) **8** was intended to elucidate the mechanism(s) by which polymers of this type might conduct electricity. In particular, it was hoped that such a study might differentiate between intrachain transport and interchain hopping as the predominant pathway for the observed conductivity in these materials.

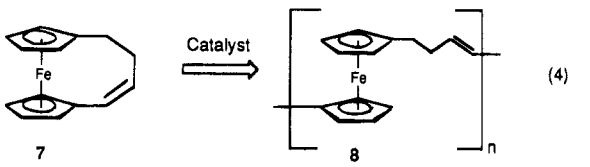

(4)

Finally, the ROMP of the monomers octamethyl-1,4-(1,1′-ferrocenediyl)-1,3-butadiene, **9**[30a] (eq 5), and 1,4-(1,1′-ferrocenediyl)-1-methoxy-1,3-butadiene, **11**[30b] (eq 6), was also studied. These monomers were synthesized in order to study the effects of substituent groups on the resultant conjugated ferrocenophane polymers. In particular, we wished to examine whether the substituents would have any effects on the solubility and/or the conductivity of these polymers. The strained nature of these species makes them very desirable candidates for ROMP, because release of ring strain drives many ROMP reactions.

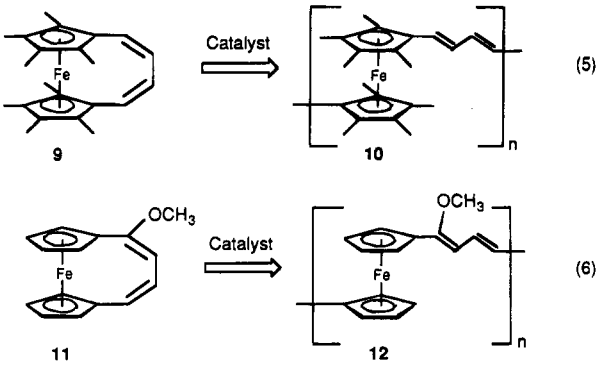

II. Results and Discussion

A. Polymerization of 5. We examined the ROMP of **5** catalyzed by **I**. Compound **5** readily polymerized at monomer:catalyst ratios of ≤50:1, even in dilute solutions at room temperature (Table 1). Polymerization could be visually followed by a color change in the solution, as red monomeric solutions became more deeply red. However, the resulting polymers were not readily soluble; poly(ferrocenylenedivinylene) (PFDV), **6**, with $n > 10$ was found to be insoluble in benzene, methylene chloride, and toluene (*vide infra*).

Polymer **6** was found to be most soluble in CH_2Cl_2. In this solvent, soluble **6** was found to have a number averaged molecular weight (M_n) of 1693 and a weight averaged molecular weight (M_w) of 2228. These values are consistent with oligomeric material with a chain length of $n = 10$. The polydispersity index (PDI) of **6** was found to be 1.3.

B. Polymerization of 7. The polymerization of **7** was found to be less facile than that of **5** (Table 2), perhaps because **7** is likely to be less strained than **5** (although we have no crystallographic evidence to support this contention). The success of the ROMP method was found to be dependent on the concentration of the monomer. Under all conditions examined, heating dilute solutions of **7** led to catalyst decomposition with no evidence of polymerization. At room temperature, concentrated solutions (≥0.4 M) with a monomer: catalyst ratio of (20–25):1, however, were found to yield polymer. The polymerization could be followed by examining the color change of the solution, as solutions were initially yellow in color, becoming tan to light orange as polymerization occurred (as judged by ^1H NMR, *vide infra*). Polymers were found to precipitate from solution within 4–12 h after initiation of polymerization. GPC characterization of the soluble material in CH_2Cl_2 showed a trimodal molecular weight distribution. Small fractions of high molecular weight and intermediate molecular weight material were produced; unfortunately, most of the chains were found to be oligomeric in nature, with a chain length of approximately 10 (molecular weight *ca.* 2574), with a PDI >6.

C. Characterization of Insoluble Polymeric Material. Insoluble polymeric material was examined by thermal gravimetric analysis (TGA), differential scanning calorimetry (DSC), elemental analysis, and solid state ^{13}C NMR spectroscopy.

1. TGA and DSC Data. The TGA and DSC spectra of the powders revealed the tendency of both **6** and **8** to lose mass at temperatures above ~250 °C (Appendix 1; Supporting Information), and a product of color similar to that of the original polymers was observed as a condensate near the heating source. These observations suggested that a large fraction of both polymers was low molecular weight material. Also, the TGA spectra of both **6** and **8** showed a slight *increase* in weight just prior to the large decrease in weight associated with mass loss. This increase is not fully understood, although it might be consistent with the reaction of the polymers with oxygen; while the TGA was performed under an argon atmosphere, sufficient oxygen is probably present under these conditions to provide a measurable increase in the weight of iron-containing polymers. An odd inconsistency between the temperatures where transitions occurred was observed between the DSC and TGA of each of the two samples. Although the TGA spectrum of **8** showed the onset of weight loss at approximately 250 °C, the DSC of the same material showed no heat flow change until approximately 385 °C. A similar trend was noted for both the TGA and DSC spectra of **6**. This behavior is not understood at present. A color change in the sample of **6** was also observed while the TGA was being performed, as the powder changed from an initial red color to a final yellow.

Elemental analyses of the polymeric material also supported the presence of a large fraction of low molecular weight material. The analytical results are reported in Table 3, along with the calculated values expected for one monomer unit of the polymers. In the preparation of these samples, benzaldehyde was used to cleave the catalysts from the ends of the polymer chains. The data shown in Table 3 suggest that the benzaldehyde end groups might contribute significantly to the total weight of the polymer chains. Thus, these results again suggest that a large fraction of the powders examined were composed of oligomeric material.

2. Solid State ^{13}C NMR Spectra. Solid state ^{13}C NMR spectra of monomer **5** and its polymer, **6**, were collected (see Supporting Information). Compound **5** displayed peaks in the region between 65 and 80 ppm due to the carbons of the cyclopentadienyl (Cp) rings, with spinning side bands occurring from −10 to +10 ppm. The olefin resonances were observed between 125 and 135 ppm. Obvious changes, consistent with polymerization, were evident in the NMR of **6** in the Cp region (figure available in the supporting information). The Cp region (65–85 ppm) and the peaks due to the olefin carbons (120–135 ppm) were broadened and slightly shifted compared to those of **5**. While the spinning side bands of the carbons in the Cp rings remained in the region from −10 to +20 ppm, new peaks, probably due to the formation of saturated carbons, appeared in the 20–40 ppm region. Although the origin of these saturated carbons remains obscure, cross-linking of the olefin moieties could be responsible for their appearance.

Solid state ^{13}C NMR spectra were also collected for compounds **7** and **8** (see Supporting Information). While the primary peaks were observed from the carbons in the Cp rings (65–85 ppm), the saturated carbons (20–35 ppm), and the olefin carbons (125–135 ppm), spinning side bands were significantly less well-resolved for **7** and **8** than in the spectra of **5** and **6**. Although the spinning side bands of the Cp region (−10 to +20 and 135–160 ppm) might be identifiable in the spectrum of **7**, the side bands due to the olefin and saturated carbons were unresolved. Again, obvious changes were evident in the breadth and number of peaks in the Cp ring (65–90 ppm), olefin (120–135 ppm), and saturated (20–40

Table 1. Polymerization of 5

catalyst	monomer:catalyst ratio	conc of **5** (M)	solvent	results and observns
I	50:1	0.41	CH_2Cl_2	oligomers; $M_n = 1693$; $M_w = 2228$
I	100:1	0.43	CH_2Cl_2	no reacn
I	50:1	2	toluene	insoluble precipitate formed; oligomers soluble in CH_2Cl_2
I	25:1	0.42	benzene	oligomeric
II	100:1	3×10^{-5}	benzene	no reacn

Table 2. Polymerization of 7

catalyst	monomer:catalyst ratio	conc of **7** (M)	solvent	results and observns
I	10:1	0.05	C_6D_6	heated to 50 °C; no reacn by NMR
I	25:1	0.43	C_6D_6	over course of 12 h formed insoluble precipitate
I	20:1	0.43	CD_2Cl_2	polymer; over course of 12 h formed flakes of precipitate
II	~10:1	~0.013	C_6D_6	heated to 65 °C; degradation of catalyst with no reacn by NMR
II	~15:1	~0.017	CD_2Cl_2	heated to 40 °C; no reacn by NMR
III	20:1	0.014–0.03	C_6D_6	room temp, 40 °C; no reacn by NMR

Table 3. Elemental Analysis of the Organic Components of Insoluble Polymers 6 and 8: Experimental *vs* Calculated Results

	% C		% H		% N	
polymer	exp	calc	exp	calc	exp	calc
6	68.55	71.22	5.22	5.12	0.08	0.00
8	66.28	70.62	5.46	5.93	0.22	0.00

Table 4. Positions of Fe($2p^3$) Peaks in XPS Spectra of Polymeric 6 and 8, Doped and Undoped, and Standards

sample	XPS Fe($2p^3$) Peak Position *vs* Carbon (eV)
undoped **6** [Fe^{2+}]	707.8
undoped **8** [Fe^{2+}]	707.8
$Me_2Fc^+BF_4^-$[Fe^{3+}]	708.5
doped **6**	707.8
doped **8**	708.1

ppm) regions of **8**, with the remaining observed peaks being spinning side bands. No evidence of cross-linking in **8** was observed; however, the presence of methylene groups in this polymer would perhaps have obscured these peaks.

Consequently, several conclusions can be drawn from these NMR data. The solid state ^{13}C NMR spectra are consistent with the formation of polymers **6** and **8** from monomers **5** and **7**. Evidence of cross-linking in **6** might be seen in the NMR data, while no evidence of cross-linking was observed in the spectrum of **8**.

D. Electrical Conductivity of Oxidatively Doped Samples. Films of I_2-doped PFDV, **6**, were found to exhibit conductivities on the order of 10^{-4} Ω^{-1} cm^{-1}, while the conductivity of doped PFB, **8**, was found to be on the order of 10^{-5} Ω^{-1} cm^{-1}. The latter polymer lacks the extended conjugation expected to be necessary for efficient intrachain mobility of charge carriers. In addition, the conductivity of the doped films of **7** was observed to be on the order of 10^{-5} Ω^{-1} cm^{-1}. The doped **5** monomer, however, exhibited no observable conductivity. Samples of all monomeric and polymeric materials were shown to be highly resistive prior to doping.

There was some question as to the lack of conductivity observed in the doped monomeric samples of **5**. The effect of oxidizing the monomers by exposure to I_2 was therefore examined in an NMR experiment with an excess of I_2 added to two NMR tubes, one containing **5** in CD_2Cl_2, the other **7** in CD_2Cl_2. The reaction between **5** and I_2 generated a copious black precipitate and a paramagnetic species (as judged by ^1H NMR). Although ferrocenium is paramagnetic, dimethylferrocenium tetrafluoroborate ($Me_2Fc^+BF_4^-$) was observed to be readily soluble in CH_2Cl_2. Thus, when potential counterion effects (i.e., I_3^- *vs* BF_4^-) upon solubility are ignored, these results suggest that **5** decomposes upon exposure to iodine. The instability of **5** to oxidation is supported by electrochemical studies (*vide infra*). Although the NMR spectrum of the solution containing **7** was observed to change upon exposure to I_2, the sample remained diamagnetic. Thus, exposure of **7** to I_2, which generated appreciable electrical conductivity, apparently did not oxidize the Fe center of the ferrocenophane.

The effects of doping by I_2 on the oxidation state of the Fe centers in the polymeric films were investigated using X-ray photoelectron spectroscopy (XPS). Films of undoped **6**, **8**, and $Me_2Fc^+BF_4^-$ were used as standards to determine the positions of the Fe($2p^3$) peaks of both oxidation states in the cyclopentadienyl environment. The positions of the peaks due to Fe($2p^3$) of all samples examined in this work are shown in Table 4. The 700 meV difference between the peak positions of Fe^{2+} and Fe^{3+} in these environments was found to be reproducible and within the resolution of these experiments. Thus, the I_2-doping of **6** was concluded to leave the Fe centers on the polymer backbone untouched within the detection limits of this technique (*i.e.*, <10% Fe oxidized). It can be concluded that the I_2 must in some way oxidize the carbon backbone of the chains, although the nature of this change could not be identified from these studies. Curiously, XPS studies of the doping of **8** by I_2 suggested partial oxidation of the Fe centers.

Attempts were also made to examine the effect of doping by I_2 on the monomeric films by XPS. Unfortunately, both monomers were found to sublime readily under the ultrahigh vacuum conditions necessary for use of this technique and our instrument did not have the capability of performing XPS measurements at low temperature.

The similarity between the conductivities of the doped polymers **6** and **8** as well as that of monomer **7** (which remained intact upon doping by I_2) argues for the importance of interchain hopping as a dominant mechanism for conductivity in these samples. Unfortunately, the high probability that only low molecular weight polymers were obtained precludes any conclusion as to whether interchain hopping would prove to be the dominant mechanism of conductivity in higher molecular weight material. In fact, the low molecular weights of these materials might have forced interchain hopping to dominate charge transport, regardless of the mech-

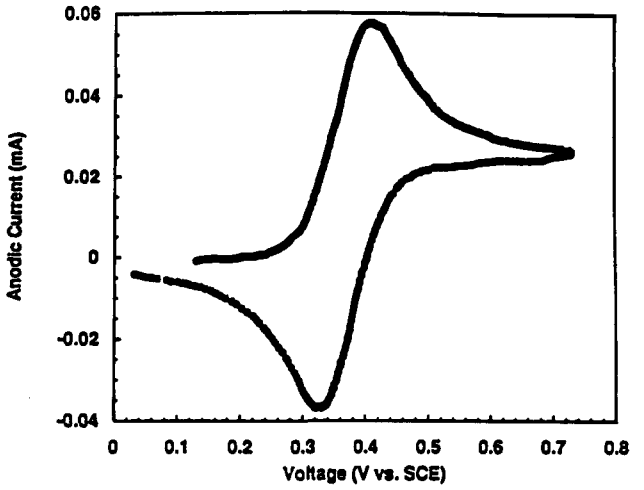

Figure 2. Cyclic voltammogram of a solution containing 1 mM **7** in 0.1 M $TMABF_4$–CH_3CN. The CV was obtained at a scan rate of 20 mV s^{-1} using a GCE working electrode with a diameter of 5.5 mm. The peak-to-peak separation observed in this voltammogram is similar to that obtained from a solution of $Fc^{+/0}$. This CV indicates reversible electrochemistry with an $E_{1/2}$ of 0.37 V *vs* SCE.

anism that would dominate the conductivity in higher molecular weight samples.

E. Electrochemistry. The electrochemistry of 1 mM solutions of monomers **5** and **7** in CH_3CN was studied. The chosen electrolyte tetramethylammonium tetrafluoroborate ($TMABF_4$) is poorly soluble in CH_3CN; however, other frequently selected electrolytes with higher solubilities have been observed to cause anomalous electrochemical behavior.[31] Cyclic voltammetry (CV) of solutions of ferrocene yielded peak-to-peak separations of 78–110 mV. The electrochemistry of **7** was shown to be reversible between potentials of −1.24 and +1.25 V *vs* SCE (Figure 2). Although the electrochemistry of **7** might have been reversible beyond +1.25 V *vs* SCE, the electrochemistry of the glassy carbon disk electrode (GCE) itself was found to interfere with measurements at more positive potentials. The electrochemical potential of this compound was determined to be $E_{1/2}$ = 0.37 V *vs* SCE.

Cyclic voltammetry of solutions containing **5** confirmed the NMR experiments on iodine exposure that showed **5** to be unstable to oxidation. The potential of solutions of **5** was cycled in these experiments between 0.03 and 0.73 V *vs* SCE. When cycled at 20 mV s^{-1} in CH_3CN, the cathodic peak current diminished relative to the anodic peak current (Figure 3). This reduction in cathodic current was believed to be the result of a further chemical reaction following oxidation of the monomer. This hypothesis was examined by obtaining cyclic voltammograms of solutions containing **5** at several scan rates, in order to determine the rate of this subsequent reaction.[32,33] The resulting data are displayed in Table 5. These data might be consistent with the presence of a chemical reaction following oxidation of **5**; however, the scatter in the resulting rate constants probably suggests a more complicated reaction sequence. The value of $E_{1/2}$ was determined to be 0.45 V *vs* SCE using data collected at a scan rate of 200 mV s^{-1}, although a ratio of cathodic peak current to anodic peak current of only 0.8 was measured at this scan rate (Figure 4). This value should be viewed in comparison with the ratios determined for **7** (0.96 at 100 mV s^{-1} and 0.99 at 20 mV s^{-1}) and for ferrocene (0.99 at both 100 and 20 mV s^{-1}) in similar experiments.

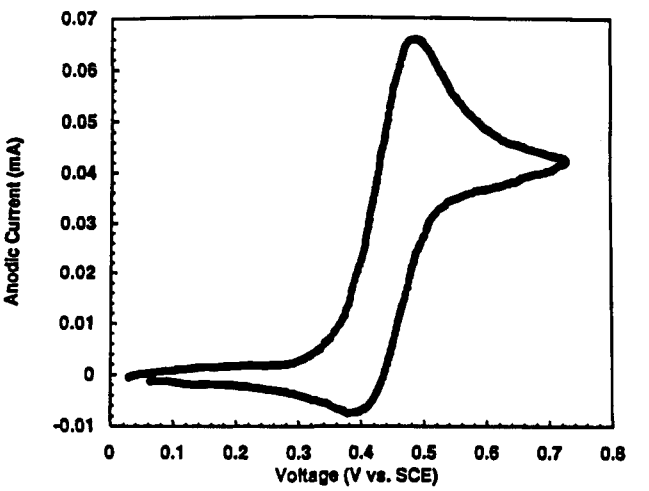

Figure 3. Cyclic voltammogram obtained at a scan rate of 20 mV s^{-1} from a 1 mM solution of **5** in 0.1 M $TMABF_4$–CH_3CN. A GCE working electrode with a diameter of 5.5 mm was used in this experiment. The lower amount of reduction current relative to the oxidation current is believed to be due to the instability of the oxidized form of **5**.

Table 5. Rate Constant Determination for the Postulated Chemical Reaction Following Oxidation of 5

scan rate (mV s^{-1})	i_c/i_a	k_f (s^{-1})
20	0.50	0.07
20	0.62	0.04
50	0.73	0.06
100	0.75	0.11
100	0.74	0.12

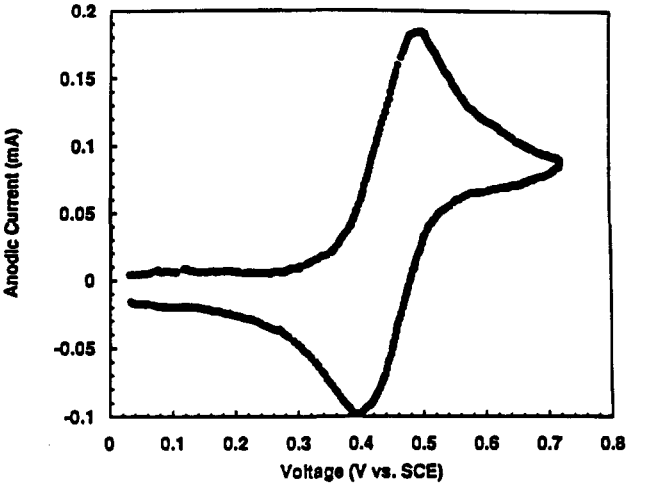

Figure 4. Cyclic voltammogram obtained at a scan rate of 200 mV s^{-1} from a 1 mM solution of **5** in 0.1 M $TMABF_4$–CH_3CN. A GCE working electrode with a diameter of 5.5 mm was used in this experiment. Although a ratio of cathodic to anodic current of only 0.8 was measured at this scan rate, an $E_{1/2}$ value of 0.45 V *vs* SCE was estimated for **5**.

As noted in the Experimental Section, the electrochemical potential of $Fc^{+/0}$ was found to be +0.40 V *vs* SCE. Thus, the electrochemical potentials of the monomers were found to bracket that of the parent ferrocene. Compound **5** was found to be less easily oxidized than ferrocene itself, while **7** was shown to be more easily oxidized.

The electrochemical properties of polymeric films have also been investigated. Unfortunately, no films of **6** were prepared that maintained their integrity during the collection of cyclic voltammograms in CH_3CN solutions.

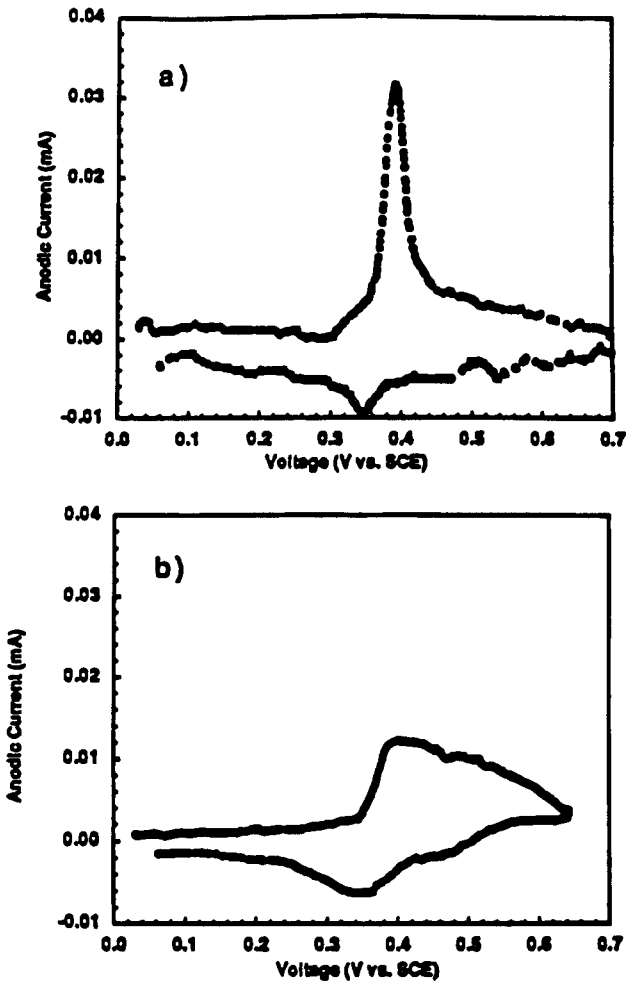

Figure 5. Cyclic voltammetry of a ~250–800 nm film of **8** on the face of a GCE working electrode with a diameter of ~2.0 mm: (a) Second complete scan. (b) Sixth complete scan. Voltammetry was performed at a scan rate of 100 mV s^{-1} in a solution of 0.1 M $TMABF_4$–CH_3CN. Notice the lower amount of anodic current in the later scan, as well as the broadening of the anodic peak.

Cyclic voltammetry of **8** was more successfully performed (Figure 5). Sharp peaks characteristic of surface-attached species were often observed on the first scan, with subsequent peaks broadening in shape. The broadening of the peaks is believed to be due to the changing nature of the film. It was concluded that the oxidation process created variations in the polymeric material, perhaps in its bonding with and proximity to the GCE electrode surface. It should be noted that the peak-to-peak separations are typically ~30 mV, which would indicate that the polymer did not dissolve as a result of the electrochemistry. In addition, mild stirring of the solution had no effect on the voltammograms. Thus, the decreasing amount of current might have been due to the destruction of the polymer. The peak-to-peak ratios for anodic and cathodic current that were measured from the CVs obtained from various samples were inconsistent. Reductive doping of films of **8** was attempted electrochemically by biasing the working electrode to a potential of −0.72 V *vs* SCE. No change in the polymer electrochemistry was observed.

F. Copolymerization Experiments. Preliminary experiments were conducted on the copolymerization of **5** and **7** with *sec*-butylcyclooctatetraene (sBuCOT). Polyacetylene polymers derived from the ROMP of sBuCOT are soluble,[19] and it was hoped that copolymerization would lend solubility to the resulting polymers, which would still have ferrocene centers as part of their backbones. Indeed, the resulting polymers were soluble in typical organic solvents (Table 6).

The copolymerization of sBuCOT/**5** in toluene produced a material having a substantially higher molecular weight than that derived exclusively from **5**. The material exhibited a bimodal molecular weight distribution (Table 6), which is often observed in polymer synthesis using ROMP.[34] An evaluation of the nature of the resulting polymer, including an analysis of whether the polymer incorporates both sBuCOT and the ferrocenophane monomers into the same chains, will be the subject of a future study.

G. Polymerization of 9 and 11. As stated in the Introduction, the polymerizations of octamethyl-1,4-(1,1′-ferrocenediyl)-1,3-butadiene, **9** (eq 5), and 1,4-(1,1′-ferrocenediyl)-1-methoxy-1,3-butadiene, **11** (eq 6), were also examined. Monomer **9** did not polymerize under any of the conditions explored in these experiments (Table 7). In contrast, the polymerization of **11** was accomplished by heating a solution of **11** with catalyst **I** to 40 °C over approximately 24 h (Table 8). Polymerization was suggested by the broadening of the peaks in the ^1H NMR spectrum, as the resultant polymer **12** was soluble in benzene (Figure 6). All glassware used in experiments involving **11** was previously treated with triethylamine, as the vinyl ether group in this compound has been reported to undergo facile hydrolysis.[30] Due to the potential hydrolysis of the vinyl ether group of **12**, further study of this polymer was not pursued at this time.

III. Conclusions

Conjugated polymers containing ferrocene moieties in their backbones, as well as an analogous unconjugated polymer, have been successfully synthesized and characterized. Although it was hoped that the ROMP of ferrocenophane monomers **5** and **7** would provide a route to the generation of high molecular weight, soluble conducting polymers, only low molecular weight materials were obtained. Both polymers **6** and **8** exhibited poor solubilities in typical organic solvents.

Conductivity studies involving polymers **6** and **8** were inconclusive, due to the likely low molecular weights of the materials. The similarity between the measured conductivities of the doped conjugated polymer **6** (10^{-4} Ω^{-1} cm^{-1}) and the doped unconjugated polymer **8** (10^{-5} Ω^{-1} cm^{-1}), as well as that of the doped monomer **7** (10^{-5} Ω^{-1} cm^{-1}), suggests that interchain hopping is the dominant mechanism of charge transport in these doped samples. It is certainly arguable, however, that intrachain transport could be found to be the dominant mechanism of transport in similar polymers of substantially longer chain lengths.

The low solubility and low conductivity reported for oligomers of poly(ferrocenylenevinylenephenylene)[4] and the low solubility reported for oligomers of poly(ferrocenylenevinylene)[35] are surprisingly similar to what we observe for oligomers of **6** and **8**. These observations suggest that the problem of solubility must be addressed (*e.g.*, by judiciously attaching appropriate substituents to the monomers) before the mechanisms of conductivity in ferrocenyl high molecular weight polymers can be understood.

The ROMP of substituted ferrocenophanes **9** and **11** was also studied. When compared to the ease with which **5** ROMPs, the failure of **9** to react under any

Table 6. Copolymerization Experiments with Ferrocenophane Monomers 5 and 7 and sBuCOT

reactants	sBuCOT: Fc monomer:catalyst ratio	conc of each monomer (M)	solvent	resulting polymer
sBuCOT/**5**/**I**	20:20:1	0.07	C_6D_6	M_n = 324; M_w = 535; PDI = 1.7
sBuCOT/**5**/**I**	40:43:1	0.65	toluene	bimodal distribution: M_n = 11 662; M_w = 24 441; PDI = 2.1 M_n = 319; M_w = 571; PDI = 1.8
sBuCOT/**7**/**I**	37:41:1	0.7	toluene	M_n = 360; M_w = 1759; PDI = 4.9

Table 7. Attempted Polymerization of 9

catalyst	monomer:catalyst ratio	conc of **9** (M)	solvent	results and observns
I	20:1	0.017	C_6D_6	heated to 60 °C; degradation of catalyst; no reacn by NMR
I	17:1	0.28	CD_2Cl_2	room temp, 40–45 °C; no reacn by NMR
II	not determined	not determined	C_6D_6	heated to 60 °C; degradation of catalyst; no reacn by NMR
III	20:1	0.02–0.04	C_6D_6	room temp, 40 °C; no reacn by NMR

Table 8. Polymerization of 11

catalyst	monomer:catalyst ratio	conc of **11** (M)	solvent	results and observns
I	10:1	0.01–0.02	C_6D_6	40 °C; no reacn by NMR
II	~10:1	~0.015–0.030	C_6D_6	40 °C for 24 h; soluble polymer
III	10:1	0.015–0.030	C_6D_6	40 °C; insoluble polymer-colloidal suspension

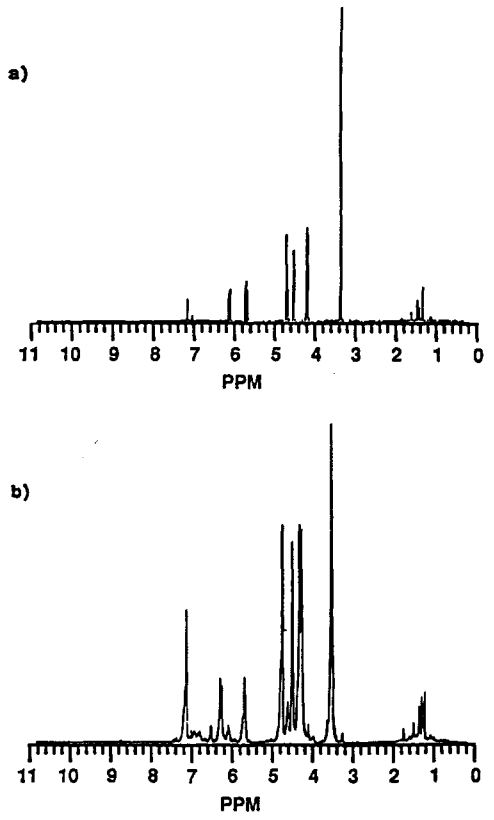

Figure 6. ^{1}H NMR spectrum of (a) **11** in C_6D_6 and (b) **12** in C_6D_6. Note the broadening of the peaks in the spectrum of the solution containing **12**. The presence of peaks due to triethylamine may be seen in the region around 1 ppm, as the NMR tube was treated to prevent hydrolysis of the methoxy group in the compounds (see ref 30).

conditions attempted in these studies suggests that steric crowding in the monomer inhibits polymerization. In addition, the difficulty observed in the ROMP of **7** vs that of **5** suggests that ring strain plays an important role in the ROMP of ferrocenophane monomers. These factors should thus be considered in future attempts to synthesize ferrocenophane monomers for related purposes. Finally, the generation of soluble polymer **12** from the ROMP of monomer **11** suggests that this system warrants further investigation.

IV. Experimental Section

A. General Procedures. The manipulations described in this work were performed in a nitrogen-filled Vacuum Atmospheres drybox, unless otherwise noted. Pentane, tetrahydrofuran, benzene, and toluene were vacuum-transferred from solutions containing sodium benzophenone ketyl. Methylene chloride and chloroform were dried with calcium hydride. All reagents were purchased from Aldrich Chemical Co. unless specified otherwise.

B. Preparation of Compounds. The 1,4-(1,1′-ferrocenediyl)-1,3-butadiene, **5**, used in these studies was synthesized using a route developed by McLaughlin *et al.*[36] The 1,4-(1,1′-ferrocenediyl)-1-butene, **7**, and monomers **9** and **11** were synthesized using a route developed by Callstrom *et al.*[30]

The three catalysts used in these studies, **I**,[37] **II**,[38] and **III**,[27] were available from previous studies and were prepared as described elsewhere.

C. Polymerizations. The extent of polymerization was monitored by ^{1}H NMR spectroscopy. These experiments were therefore performed in an NMR tube with a monomer and a catalyst dissolved in a deuterated solvent. Polymerization was confirmed by disappearance of the monomer and broadening or shifting of the peaks observed in the ^{1}H NMR spectra of the solutions.

Bulk polymerizations were carried out by combining monomer and catalyst in a vial, followed by addition of the appropriate solvent. These polymerizations were monitored by color and viscosity changes in the solution. Following polymerization, 1–2 drops of benzaldehyde were added to each solution to end-cap the polymers.[17] GPC samples (3–5 mg mL^{-1}) were filtered through a 0.5 μm filter prior to injection into the chromatograph.

Copolymerization experiments were performed in a manner similar to those described above, except that two monomers were added to the reaction vessel before the catalyst and solvent were added. It should be noted, however, that *sec*-butylcyclooctatetraene (sBuCOT) is a liquid at room temperature, in contrast to the solid ferrocenophane monomers. In addition, only catalyst **I** was used in the copolymerization experiments.

Samples of insoluble polymeric material were also prepared for characterization. Solutions of monomer and catalyst **I** (~45:1 monomer:catalyst ratios) were stirred for 46 h. The formation of a precipitate was observed in the solution containing **5** within minutes, while a precipitate was found in the solution of **7** after approximately 8 h. After 46 h, the volume of the solution containing **7** was then reduced by two-thirds and the slurry stirred for another hour before a drop of benzaldehyde was added to each solution. After stirring for 30 min, the slurries were each precipitated into pentane. The

precipitates were then washed twice with pentane and twice with hexane. A yellow powder was obtained from the solution of **7**, while a red powder was obtained from the solution containing **5**. These powders were examined as described below.

D. Polymer Characterization. As noted above, soluble polymers were characterized by ^1H NMR spectroscopy and gel permeation chromatography (GPC). Proton NMR spectra were recorded on a 300 MHz General Electric QE spectrometer. Proton chemical shifts are reported as referenced to internal solvent protons. GPC was performed on one of two instruments: either a homemade instrument with three Shodex size exclusion columns, model numbers KF-803, KF-804, and KF-805 (70 000, 400 000, and 4 000 000 MW polystyrene exclusion limit, respectively), an Altex model 110A pump, a Kratos Analytical Instruments Spectroflow 757 absorbance detector, and a Knauer differential refractometer, with CH_2Cl_2 as the eluant at a flow rate of 1.5 mL min^{-1}, or a Waters GPC-120C with THF as the eluant at a flow rate of 1.0 mL min^{-1}. Molecular weights were determined relative to polystyrene standards.

Insoluble polymeric materials were characterized by solid state ^{13}C NMR spectroscopy, thermal gravimetric analysis (TGA), differential scanning calorimetry (DSC), and elemental analysis. The solid state ^{13}C NMR spectra were obtained using a Bruker MSL-200 spectrometer. The TGA and DSC measurements were obtained using a Perkin-Elmer PC series TGA7 and DSC7, respectively, in covered but not sealed pans. Both thermal analyses were carried out by heating samples under an argon flush in covered pans in a Pt sample holder. Samples were heated from an initial temperature of 50 °C to a final temperature of 600 °C. Although the temperature ramp rate was typically 20 °C min^{-1}, a ramp rate of 10 °C min^{-1} was also utilized, with no difference observed in the resulting data. Conventional percent weight loss *vs* temperature and heat flow *vs* temperature profiles were obtained using PC Series Multitasking Version 2.1. IR spectra of **5**–**8** were obtained on a Perkin-Elmer 1600 Series FTIR spectrometer using KBr pellets (Appendix 2; Supporting Information). Elemental analyses of both polymers were obtained from Oneida Research Services, Inc.

E. Preparation of Films. Polymeric films were cast by simultaneous deposition of solutions containing monomer and catalyst **I** on a glass slide.[39] Alternatively, solutions containing monomer and catalyst were allowed to react before being transferred to a glass slide. Since the concentrations did not seem to affect the resulting conductivity measurements of **6**, solution concentrations ranging from 0.2 to 1.4 M were used. Monomer:catalyst ratios were generally maintained at either 25:1 or 50:1, since higher ratios did not lead to polymerization. As discussed in the Results and Discussion, solution concentrations did appear to be an important variable in the polymerization of **7**, so solutions were prepared at concentrations of 0.4–0.5 M. Monomeric films were cast by depositing solutions of monomer (*ca.* 0.4 M) dropwise on a glass slide.

F. Oxidative Doping of Films. Films were oxidized by exposure to I_2 vapor in a previously evacuated chamber, followed by removal of excess I_2 by exposure to dynamic vacuum. Although variable amounts of I_2 exposure were investigated, all measurements reported in this work resulted from exposure periods of 1 h, followed by 20–30 min of exposure to vacuum. Variability in this regimen had no apparent effect on the resulting conductivity. In all cases, exposure of the colored films to iodine yielded blue-black and extremely brittle samples.

G. Thickness and Conductivity Measurements. Thickness measurements of the conducting films were made with a Fowler Digitrix II micrometer. Sample thicknesses of the polymeric films prepared for electrochemistry were measured using a Dektak 3030a profilometer. The conductivities of the films were investigated using an osmium-tipped four-point probe with probe spacings of 1.27 mm. Current was supplied using an EG & G Princeton Applied Research Model 173 potentiostat/galvanostat in the galvanostat setting and a Model 175 universal programmer. The small applied currents (typically 0.02–0.40 μA) were measured using a Fluke 8060 A True RMS multimeter in series with the four-point probe. Resulting voltages were measured with either a Fluke 8060 A True RMS multimeter or a Fluke 8024 B multimeter in parallel with the probe. The resulting data were interpreted as described in ref 40.

The polymeric nature of the films used in these experiments was examined by several methods. A set of experiments was performed in which films of **6** and **8** were rinsed with pentane prior to doping. The conductivities of these rinsed films were compared with those of films that were not rinsed, with no obvious changes arising from this procedure. Additionally, in most cases, no color was seen in the rinsed pentane, indicating that very little monomer, if any, remained in the films after the reaction. Moreover, it was sometimes possible to remove the undoped films from the glass slides in a single sheet, a test which often indicates the presence of high molecular weight material.

H. X-ray Photoelectron Spectroscopy. X-ray photoelectron spectroscopy (XPS) data were obtained on polymeric films that were prepared as in the previous conductivity experiments. The conductivities of the films were determined before XPS studies were carried out, with typical conductivity values resulting. A Surface Science Instruments M-Probe instrument was used to obtain XPS spectra, which were then analyzed using the provided software package, M-Probe ESCA. The excitation source was an Al Kα line equipped with a monochromator. A spot size of 400 × 1000 μm was used with an electron energy analyzer pass energy of 150 V, resulting in low-resolution scans. Due to excessive outgassing of the samples in the ultrahigh vacuum environment, more detailed scans, requiring longer accumulation times, could not be acquired. Surface charging of the samples was observed during the XPS experiments, due to the relatively insulating nature of the films. A flood gun emitting electrons at an energy of 1 V was used in order to neutralize this effect. Due to this surface charging, the XPS spectra were observed to shift relative to an absolute reference. The peak due to Fe($2p^3$) was therefore referenced versus the binding energy of adventitious carbon (284.6 eV).

I. Electrochemistry. Electrometric grade tetrakis(*n*-butyl)ammonium tetrafluoroborate ($TBABF_4$) (recrystallized from 3:1 by volume water:methanol) and tetramethylammonium tetrafluoroborate ($TMABF_4$) (recrystallized from acetonitrile and ethyl acetate) were used as electrolytes, purchased from Southwestern Analytic Chemicals Inc. and Aldrich. After recrystallization, these electrolytes were dried by heating to 80 °C for >36 h *in vacuo*. The ferrocene used in these experiments was available from previous experiments and had been sublimed. Acetonitrile was distilled from CaH_2 and then from P_2O_5 (≤0.5 g/1000 mL of CH_3CN). The solvent was transferred to a dried round bottom flask, stored over 4 Å molecular sieves, and filtered though 1.0 μm filters before use.

All electrochemical measurements were performed using an EG & G Princeton Applied Research Model 173 potentiostat/galvanostat and Model 175 universal programmer. Voltammograms were recorded using a Houston Instrument Omnigraphic 2000 chart recorder.

Cyclic voltammetry was performed using a three-electrode configuration in a one-compartment cell. The working electrode used in these experiments was a glassy carbon disk electrode (GCE) with a diameter of either 5.5 or ~2.0 mm, unless otherwise noted. A 3.78 cm^2 Pt foil served as the counter electrode in these experiments. A quasi-reference electrode was used, made up of a silver wire immersed into a solution of 0.1 M $TBABF_4$ with a pinch of $AgNO_3$ in CH_3CN and separated from the cell with a Corning Glass Vycor frit. The reference electrode was regularly calibrated against the ferrocene/ferrocenium couple in 0.1 M $TMABF_4$–CH_3CN.

Cyclic voltammograms of polymeric films and 1 mM solutions of monomers **5** and **7** were collected in 0.1 M solutions of $TMABF_4$ in CH_3CN. Solutions containing **7** and catalyst **I** (≤25:1 monomer:catalyst ratio, ~0.4 M) were allowed to polymerize for ≥3 h, while solutions of **5** and catalyst **I** (≤50:1, ~0.2 M) were given up to 22 h for polymerization to occur. Solutions were then diluted to a concentration of 0.5 mg mL^{-1}. About 10 μL of either solution was deposited *via* syringe onto

the face of a GCE. Thickness characterization (executed using a profilometer) on similarly prepared films showed thicknesses of 250–800 nm.

The electrochemical potentials that were obtained as described above were converted to the same scale as the standard calomel electrode (SCE) using the value of $E°(Fc^+/Fc) = 0.40$ V *vs* SCE. This value was determined experimentally by cyclic voltammetry performed in air, although similar care was taken in preparing the solvent and electrolyte used in these experiments as for experiments performed in the drybox. The cyclic voltammetry was performed in a three-electrode configuration in a one-compartment cell; however, the reference electrode used in this case was a silver wire immersed in saturated LiCl in CH_3CN inside a glass tube separated from the cell by a Corning Glass Vycor frit. The electrode was left sitting in saturated LiCl in CH_3CN overnight before use. This reference electrode was regularly calibrated against a commercially prepared SCE (Fisher). Both a 5.5 mm diameter GCE and a 2.0 mm diameter Pt disk electrode were used interchangeably as the working electrode in these experiments.

Acknowledgment. We acknowledge the National Science Foundation, grant CHE-9202583, for support of this work. T.R.L. wishes to thank the NIH for a Postdoctoral Fellowship (GM14688-02). We thank Dr. Robert Lee for assistance in obtaining and analyzing the solid state ^{13}C NMR spectra, Marc Hillmyer for performing the TGA and DSC measurements, and Dr. Iver Lauermann for obtaining the XPS spectra.

Supporting Information Available: TGA, DSC, IR, and NMR spectra of **5**–**8** (11 pages). This material is contained in many libraries on microfiche, immediately follows this article in the microfilm version of the journal, can be ordered from the American Chemical Society, and can be downloaded from the Internet; see any current masthead page for ordering information and Internet access instructions.

References and Notes

(1) Marks, T. J. *Science* **1985**, *227*, 881.
(2) Sailor, M. J.; Ginsberg, E. J.; Gorman, C. B.; Kumar, A.; Grubbs, R. H.; Lewis, N. S. *Science* **1990**, *249*, 1146.
(3) Fox, M. A.; Chandler, D. A. *Adv. Mater.* **1991**, *3*, 381.
(4) Chien *et al.* have reported the synthesis of soluble oligomers of poly(ferrocenylenevinylenephenylenevinylene) using Wittig chemistry: Gooding, R.; Lillya, C. P.; Chien, J. C. W. *J. Chem. Soc., Chem. Commun.* **1983**, 151.
(5) Cotton, F. A.; Wilkinson, G. *Advanced Inorganic Chemistry*; Wiley: New York, 1980.
(6) Scholl, H.; Sochaj, K. *Electrochim. Acta* **1991**, *36*, 689.
(7) Foucher, D. A.; Tang, B. Z.; Manners, I. *J. Am. Chem. Soc.* **1992**, *114*, 6246.
(8) (a) Foucher, D. A.; Ziembinski, R.; Tang, B. Z.; Macdonald, P. M.; Massey, J.; Jaeger, R.; Vancso, G. J.; Manners, I. *Macromolecules* **1993**, *26*, 2878. (b) Foucher, D.; Ziembinski, R.; Petersen, R.; Pudelski, J.; Edwards, M.; Ni, Y.; Massey, J.; Jaeger, C. R.; Vancso, G. J.; Manners, I. *Macromolecules* **1994**, *27*, 3992.
(9) Finckh, W.; Tang, B. Z.; Foucher, D. A.; Zamble, D. B.; Lough, A.; Manners, I. *Organometallics* **1993**, *12*, 823.
(10) Tang, B. Z.; Petersen, R.; Foucher, D. A.; Lough, A.; Coombs, N.; Sodhi, R.; Manners, I. *J. Chem. Soc., Chem. Commun.* **1993**, 523.
(11) Ziembinski, R.; Honeyman, C.; Mourad, O.; Foucher, D. A.; Rulkens, R.; Liang, M.; Ni, Y. *Phosphorus, Sulfur, Silicon, Relat. Elem.* **1993**, *76*, 219.
(12) Foucher, D. A.; Petersen, R.; Tang, B. Z.; Ziembinski, R.; Coombs, N.; Macdonald, P. M.; Sodhi, R. N. S.; Massey, J.; Vancso, G. J.; Manners, I. *Polym. Prepr. (Am. Chem. Soc., Div. Polym. Chem.)* **1993**, *34*, 328.
(13) Honeyman, C.; Foucher, D. A.; Mourad, O.; Rulkens, R.; Manners, I. *Polym. Prepr. (Am. Chem. Soc., Div. Polym. Chem.)* **1993**, *34*, 330.
(14) Foucher, D. A.; Manners, I. *Makromol. Chem., Rapid Commun.* **1993**, *14*, 63.
(15) Nguyen, M. T.; Diaz, A. F.; Dement'ev, V. V.; Pannell, K. H. *Chem. Mater.* **1993**, *5*, 1389.
(16) (a) Dement'ev, V. V.; Cervantes-Lee, F.; Parkanyi, L.; Sharma, H.; Pannell, K. H.; Nguyen, M. T.; Diaz, A. *Organometallics* **1993**, *12*, 1983. (b) Pannell, K. H.; Dementiev, V. V.; Li, H.; Cervantes-Lee, F.; Nguyen, M. T.; Diaz, A. F. *Organometallics* **1994**, *13*, 3644.
(17) Nguyen, M. T.; Diaz, A. F.; Dement'ev, V. V.; Pannell, K. H. *Chem. Mater.* **1994**, *6*, 952.
(18) Nelson, J. M.; Rengel, H.; Manners, I. *J. Am. Chem. Soc.* **1993**, *115*, 7035.
(19) Gorman, C. B. Ph.D. Thesis, California Institute of Technology, 1992.
(20) Grubbs, R. H.; Tumas, W. *Science* **1989**, *243*, 907.
(21) Gilliom, L. R.; Grubbs, R. H. *J. Am. Chem. Soc.* **1986**, *108*, 733.
(22) Wallace, K. C.; Schrock, R. R. *Macromolecules* **1987**, *20*, 448.
(23) Schrock, R. R.; Feldman, J.; Cannizzo, L. F.; Grubbs, R. H. *Macromolecules* **1987**, *20*, 1169.
(24) Murdzek, J. S.; Schrock, R. R. *Macromolecules* **1987**, *20*, 2640.
(25) Novak, B. M.; Grubbs, R. H. *J. Am. Chem. Soc.* **1988**, *110*, 7542.
(26) Novak, B. M.; Grubbs, R. H. *J. Am. Chem. Soc.* **1988**, *110*, 960.
(27) Nguyen, S. T.; Johnson, L. K.; Grubbs, R. H.; Ziller, J. W. *J. Am. Chem. Soc.* **1992**, *114*, 3974.
(28) (a) Cannizzo, L. F.; Grubbs, R. H. *Macromolecules* **1988**, *21*, 1961. (b) Risse, W.; Wheeler, D. R.; Cannizzo, L. F.; Grubbs, R. H. *Macromolecules* **1989**, *22*, 3205.
(29) Schrock, R. R.; Krouse, S. A.; Knoll, K.; Feldman, J.; Murdzek, J. S.; Yang, D. C. *J. Mol. Catal.* **1988**, *46*, 243.
(30) (a) Pudelski, J. K.; Callstrom, M. R. *Organometallics* **1994**, *13*, 3095. (b) Pudelski, J. K.; Callstrom, M. R. *Organometallics* **1992**, *11*, 2757.
(31) Jozefiak, T. H.; Ginsburg, E. J.; Gorman, C. B.; Grubbs, R. H.; Lewis, N. S. *J. Am. Chem. Soc.* **1993**, *115*, 4705.
(32) Nicholson, R. S.; Shain, I. *Anal. Chem.* **1964**, *36*, 706.
(33) Bard, A. J.; Faulkner, L. R. *Electrochemical Methods: Fundamentals and Applications*; Wiley: New York, 1980.
(34) See, for example: Schimetta, M.; Stelzer, F. *Macromolecules* **1994**, *27*, 3769.
(35) Gamble, A. S., Patton, J. T., Boncella, J. M. *Makromol. Chem., Rapid Commun.* **1992**, *13*, 109.
(36) Erickson, M. S.; Fronczek, F. R.; McLaughlin, M. L. *Tetrahedron Lett.* **1993**, *34*, 197.
(37) Johnson, L. K.; Virgil, S. C.; Grubbs, R. H.; Ziller, J. W. *J. Am. Chem. Soc.* **1990**, *112*, 5384.
(38) Schrock, R. R.; DePue, R. T.; Feldman, J.; Schaverien, C. J.; Dewan, J. C.; Liu, A. H. *J. Am. Chem. Soc.* **1988**, *110*, 1423.
(39) Klavetter, F. L. Ph.D. Thesis, California Institute of Technology, 1992.
(40) Sze, S. M. *Physics of Semiconductor Devices*; Wiley: New York, 1981.

MA950910E